SUBMITTED TO APJ LETTERS
Preprint typeset using LaTeX style emulateapj v. 03/07/07

# THE RELATION OF $H\alpha$ EMISSION AND RADIO SOURCES TO INTRACLUSTER GAS ENTROPY IN GALAXY CLUSTERS

KENNETH W. CAVAGNOLO[1,2], MEGAN DONAHUE[1], G. MARK VOIT[1], AND MING SUN[1]

*April 10, 2008*

## ABSTRACT

We present results from a *Chandra* archival study of the intracluster entropy distribution for a sample of 217 galaxy clusters showing that $H\alpha$ and radio emission from the brightest cluster galaxy are sensitive to gas entropy of the cluster core. After parameterizing the central entropy, $K_0$, of each cluster as the value at which the entropy distribution departs from a power-law, we compare the $K_0$ values with the $H\alpha$ luminosities and radio powers of the brightest cluster galaxies. Interpreting these $H\alpha$ and radio emission as indicators that star formation and/or AGN are active in the BCG, we find that for most clusters with $K_0 \lesssim 30$ keV cm$^2$ galactic feedback is active, while above this threshold the feedback is significantly fainter and in most clusters not detected.

*Subject headings:* galaxies: clusters: general – X-rays: active – galaxies: conduction – galaxies: cooling flows – galaxies

## 1. INTRODUCTION

In recent years the "cooling flow problem" has been the focus of intense scrutiny as the solutions have broad impact in the area of galaxy formation. The adiabatic model of hierarchical structure formation predicts an over-production of dwarf and massive galaxy haloes, and that the most massive galaxies in the Universe – brightest cluster galaxies (BCGs) – should be bluer and more massive than observations find. Compounding this issue is that star formation in massive galaxies was more prodigious at higher redshifts (Cowie et al. 1996; Juneau et al. 2005), contradicting model ~~predictions and resulting in the observation of present-day ellipticals being "dead and red". There is also the so-called cosmic downsizing problem (Cowie et al. 1996), where massive galaxies are observed to form earlier than hierarchical galaxy formation models predict.~~ It has been hypothesized that ~~these~~ problems with the existing galaxy formation models are related to galactic feedback, specifically in the form of active galactic nuclei (AGN) and star formation/supernovae. Both theoretical (Bower et al. 2006; Croton et al. 2006) and observational (see McNamara & Nulsen 2007 for a review) studies have given this hypothesis considerable traction in recent years.

Studies which seek to explain the differences between galaxy formation models and observations by investigating the interaction of feedback sources with the hot atmosphere of their host galaxy cluster have thus far been fruitful. Using properties of X-ray cavities in the intracluster medium (ICM) in combination with the energetics of the BCG radio source, Bîrzan et al. (2004) observed that AGN feedback provides the necessary energy to retard cooling in the cores of clusters. This result suggests that, under the right conditions, AGN are capable of quenching star formation by heating the surrounding ICM. One quantity which has proven useful in studying AGN heating is ICM entropy.

In previous observational work we have focused on ICM entropy as a means for understanding the cooling and heating processes in clusters (see Donahue et al. 2005, 2006; Cavagnolo et al. 2008a). Entropy, $K = P\rho^{-2/3}$, is useful as it is a more fundamental property of the ICM than temperature or density alone (Voit et al. 2002; Voit 2005). ICM temperature mainly reflects the depth and shape of the dark matter potential well, while density represents how much the gravitational well can compress the gas. Entropy on the other hand determines the density of an isobaric gas parcel, and only gains or losses of heat ~~energy~~ can change the entropy. Thus, study of the ICM entropy distribution is an investigation of the cluster thermal history.

In Cavagnolo et al. (2008a) we present the radial entropy profiles for a sample of 217 clusters taken from the *Chandra* Data Archive. We have named this project the Archive of Chandra Cluster Entropy Profile Tables, or *ACCEPT* for short. To characterize the ICM entropy distributions of *ACCEPT* we fit the equation $K(r) = K_0 + K_{100}(r/100\ \mathrm{kpc})^{\alpha}$ to each entropy profile. In this equation, ~~$K_0$ is the central entropy and~~ $K_{100}$ is a normalization of the power-law component at 100 kpc. $K_0$ is not the minimum core entropy or the entropy at $r = 0$, nor is it the gas entropy which would be measured immediately around the AGN or in a BCG X-ray coronae. $K_0$ ~~simply~~ parameterizes the departure of the radial entropy distribution from a power-law. ~~There are two results in~~ Cavagnolo et al. (2008a) ~~which are relevant to this letter; 1)~~ $K_0$ is non-zero for most clusters in *ACCEPT* and ~~2)~~ the $K_0$ distribution is bimodal.

In this letter we present the results of exploring the relationship between the expected by-products of cooling, *e.g.* star formation and AGN activity, to the $K_0$ values for the clusters in *ACCEPT*. To determine the activity level of feedback in cluster cores, we selected two readily available observables: $H\alpha$ and radio emission. Using these observables as a window on the processes operating in the core of clusters, we find there exists a critical entropy level below which $H\alpha$ and radio emission are predominantly present, while above this threshold these emission sources are much fainter and in most cases are not detected. Our results suggest the formation of thermal instabilities in the ICM, and initiation of processes such as star formation and AGN activity, are connected to core entropy.

This letter proceeds in the following manner: In §2 we cover the basics of our data analysis. The entropy-$H\alpha$ relationship is discussed in §3, while the entropy-radio relationship is discussed in §4. A brief summary is provided in §5.

[1] Michigan State University, Department of Physics and Astronomy, BPS Building, East Lansing, MI 48824
[2] cavagnolo@pa.msu.edu

For this letter we have assumed a flat ΛCDM Universe with cosmogony $\Omega_M = 0.3$, $\Omega_\Lambda = 0.7$, and $H_0 = 70$ km s$^{-1}$ Mpc$^{-1}$. All uncertainties are 90% confidence.

## 2. DATA ANALYSIS

In this letter we briefly describe our data reduction and methods for producing entropy profiles and refer interested readers to the more thorough explanations in Donahue et al. (2006), Cavagnolo et al. (2008a), and Cavagnolo et al. (2008b).

### 2.1. *X-ray*

X-ray data was taken from publicly available observations in the *Chandra* Data Archive. Following standard CIAO reduction techniques[3], data was reprocessed using CIAO 3.4.1 and CALDB 3.4.0, resulting in point source and flare clean events files at level-2. Entropy profiles were derived using the relation $K(r) = T(r)n_e(r)^{-2/3}$ where $T(r)$ is the radial ICM temperature and $n_e(r)$ is the radial ICM electron density.

Radial temperature profiles were created by ~~spatially~~ dividing each cluster into concentric annuli with the ~~minimum~~ requirement of three annuli containing 2500 counts. Source spectra were extracted from these annuli, while corresponding background spectra were extracted from blank-sky backgrounds tailored to match each observation. Each blank-sky background was corrected to account for variation of the hard-particle background, while spatial variation of the soft-galactic background was accounted for through addition of a fixed background component during spectral fitting. Weighted responses which account for spatial variations of the CCD calibration were also created for each observation. Spectra were then fit over the energy range 0.7-7.0 keV in XSPEC 11.3.2ag (Arnaud 1996) using a single-component absorbed thermal model.

Radial electron density profiles were created using surface brightness profiles and spectroscopic information. Exposure-corrected, background-subtracted, point-source-clean surface brightness profiles were extracted from 5″ concentric annular bins over the energy range 0.7-2.0 keV. In conjunction with the spectroscopic normalization and 0.7-2.0 keV count rate, surface brightness was converted to electron density using the deprojection technique of Kriss et al. (1983). Errors were estimated using 5000 Monte Carlo realizations of the surface brightness profile.

A radial entropy profile for each cluster was then produced from the temperature and electron density profiles. The entropy profiles were fit with a hybrid model which is a power-law at large radii and can flatten at small radii (see §1 for equation). We define central entropy as $K_0$ from the best-fit model. In Cavagnolo et al. (2008a) we demonstrate that the best-fit $K_0$ and observational $K_0$ do not significantly differ for most clusters. ~~As noted in Section 1, $K_0$ is not the minimum gas entropy found in the core, nor does it represent an absolute flattening of the profile. Rather $K_0$ is a characterization of the entropy distribution's departure from a power-law, and is a representation of the azimuthally averaged entropy for the innermost radial bins.~~

### 2.2. $H\alpha$

One goal of our project was to determine if ICM entropy is connected to processes like star formation. Thus, we selected $H\alpha$ emission, which has proven to be a strong indicator of ongoing star formation (Kennicutt 1983), to facilitate investigation of possible connections between entropy and star formation.

We have gathered $H\alpha$ values from several sources, most notably Crawford et al. (1999). Additional sources of data are M. Donahue's observations while at Carnegie, Heckman et al. (1989), Donahue et al. (1992), Lawrence et al. (1996), Valluri & Anupama (1996), White et al. (1997), Crawford et al. (2005), and Quillen et al. (2007). To place all the $H\alpha$ measurements on equal footing, we have rolled back from the cosmogony used in each study and re-calculated $H\alpha$ luminosities using our assumed ΛCDM values.

The $L_{H\alpha}$ values shown in this letter are not meant to be interpreted as a surrogate for star formation rates, *e.g.* using the Kennicutt relation. The ~~individual values~~ of $L_{H\alpha}$ are not important for the purposes of this letter and we suggest the reader interpret the $L_{H\alpha}$ values as a binary indicator: either $H\alpha$ emission is ~~off or on~~.

### 2.3. *Radio*

We were also interested to know if ICM entropy is connected to AGN activity. It has long been known that BCGs are more likely to ~~house~~ radio-loud AGN than other cluster galaxies (Burns et al. 1981; Valentijn & Bijleveld 1983; Burns 1990). Thus, we chose to look for radio emission from the BCG of each *ACCEPT* cluster as a sign that an AGN was active in the cluster core.

We take advantage of the nearly all-sky flux-limited coverage of the NRAO VLA Sky Survey (NVSS, Condon et al. 1998) and Sydney University Molonglo Sky Survey (SUMSS, Bock et al. 1999; Mauch et al. 2003). Both surveys probe very low radio fluxes ~~and are excellent for our purposes~~. NVSS is a continuum survey at 1.4 GHz of the entire sky north of $\delta = -40°$, while SUMSS is a continuum survey at 843 MHz of the entire sky south of $\delta = -30°$. The completeness limit of NVSS is $\approx 2.5$ mJy and for SUMSS it is $\approx 10$ mJy when $\delta > -50°$ or $\approx 6$ mJy when $\delta \leq -50°$. The NVSS positional uncertainty for both right ascension and declination is $\lesssim 1''$ for sources brighter than 15 mJy, and $\approx 7''$ at the survey detection limit (Condon et al. 1998). At $z = 0.2$, these uncertainties equal distances on the sky of $\sim 3-20$ kpc. For SUMSS, the positional uncertainty is $\lesssim 2''$ for sources brighter than 20 mJy, and is always less than $10''$ (Bock et al. 1999; Mauch et al. 2003). The distances at $z = 0.2$ associated with these uncertainties is $\sim 6-30$ kpc. We calculate the radio power for each radio source using the standard relation $\nu L_\nu = 4\pi D_L^2 S_\nu f_0$ where $S_\nu$ is the 1.4 GHz or 843 MHz flux from NVSS or SUMSS, $D_L$ is the luminosity distance, and $f_0$ is the central beam frequency of the observations.

Radio sources were found using two methods. The first method was to search for sources within a fixed angular distance of $20''$ around the cluster X-ray peak. The probability of randomly finding a radio source within an aperture of $20''$ is exceedingly low ($< 0.004$ for NVSS). Thus, in 217 total field searches, we expect to find no more than one spurious source. The second method involved searching for sources within 20 kpc of the cluster X-ray peak. At $z \approx 0.051$, $1''$ equals 1 kpc, thus for clusters at $z \gtrsim 0.05$ the 20 kpc aperture is smaller than the $20''$ aperture and the likelihood of finding a spurious source gets smaller. Both methods produce nearly the same list of radio sources with the differences being the very large, extended lobes of low-redshift radio sources such as Hydra A.

[3] http://cxc.harvard.edu/ciao/guides/

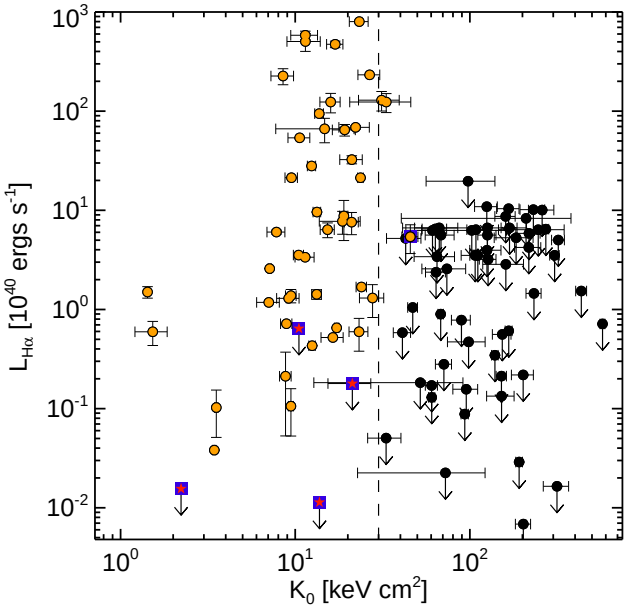


FIG. 1.— Plotted here is central entropy versus $H\alpha$ luminosity. Orange circles represent detections, black circles are non-detection upper-limits, and blue boxes with inset red stars or orange circles are peculiar clusters which do not adhere to the observed trend (see text). The vertical dashed line marks $K_0$ = 30 keV cm$^2$. Note the presence of an $H\alpha$ detection dichotomy starting at $K_0 \lesssim 30$ keV cm$^2$.

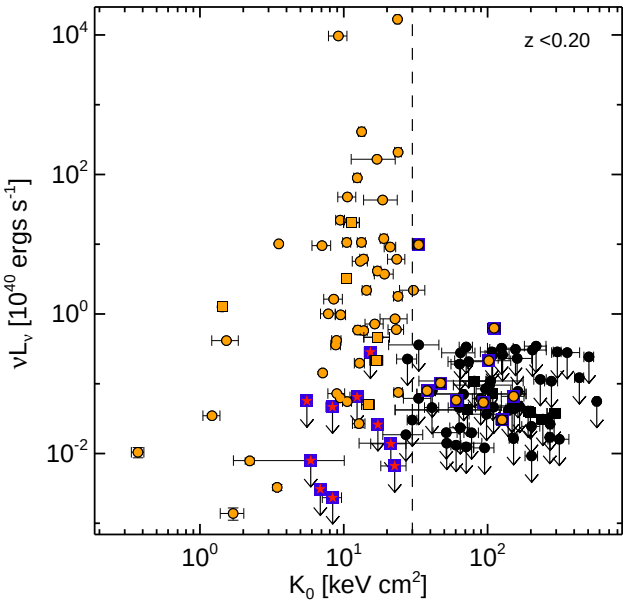


FIG. 2.— Shown is BCG associated radio power versus $K_0$ for clusters with $z < 0.2$. Orange points represent detections, black points are non-detection upper-limits, and blue boxes with inset red stars or orange points are peculiar clusters which do not adhere to the observed trend (see text). Circles are for NVSS observations and squares are for SUMSS observations. The vertical dashed line marks $K_0$ = 30 keV cm$^2$. The radio sources show the same trend as $H\alpha$: for $K_0 \lesssim 30$ keV cm$^2$ bright radio emission is preferentially "on".

To make a spatial and morphological assessment of the radio emission's origins, *i.e.* determining if the radio emission is associated with the BCG, high angular resolution is necessary. However, NVSS and SUMSS are low-resolution surveys with FWHM at $\approx 45''$. We therefore cannot distinguish between ghost cavities/relics, extended lobes, point sources, re-accelerated regions, or if the emission is coming from a galaxy very near the BCG or a background/foreground source. We have handled this complication by visually inspecting each radio source in relation to the optical (using DSS I/II) and infrared (using 2MASS) emission of the BCG. We have used this method to establish that the radio emission is most likely coming from the BCG. When available, high resolution data from VLA FIRST[4] was added to the visual inspection.

## 3. $H\alpha$ EMISSION AND CENTRAL ENTROPY

Of the 217 clusters in *ACCEPT*, we located $H\alpha$ observations from the literature for 105 clusters. Of those 105, $H\alpha$ was detected in 45, while the remaining 60 have ~~no detection. We treat the non-detections as upper limits using the observation's flux limit.~~ The mean central entropy for clusters with detections is $K_0 = 14.1 \pm 4.9$ keV cm$^2$, and for clusters with only upper-limits $K_0 = 124 \pm 47$ keV cm$^2$.

In Figure 1 central entropy is plotted versus $H\alpha$ luminosity. One can immediately see there is a dichotomy between clusters with and without $H\alpha$ emission. If a cluster has a central entropy $\lesssim 30$ keV cm$^2$ then $H\alpha$ emission is "on", while above this threshold the emission is predominantly "off". For brevity we refer to this threshold as $K_{\rm thresh}$ hereafter. The cluster above $K_{\rm thresh}$ which has $H\alpha$ emission (blue box with orange dot) is Zwicky 2701 ($K_0 = 45.6 \pm 4.8$ keV cm$^2$). There are also clusters below $K_{\rm thresh}$ without $H\alpha$ emission (blue boxes with red stars): A2029, A2107, EXO 0422-086, and RBS 533. These five clusters are clearly exceptions to the much larger trend.

The entropy threshold we observe is also insensitive to redshift effects, *i.e.* $H\alpha$ emission unaccounted for in high or low redshifts galaxies will not change our results. The mean and dispersion of the redshifts for clusters with and without $H\alpha$ are nearly identical, $z = 0.126 \pm 0.106$ and $z = 0.136 \pm 0.084$ respectively, and applying a redshift cut (*i.e.* $z = 0 - 0.15$ or $z = 0.15 - 0.3$) does not change the $K_0$-$H\alpha$ dichotomy. Most important is that changes in the $H\alpha$ luminosities will ~~only~~ move points up or down in Figure 1, mobility along the $K_0$ axis is minimal. Qualitatively, the correlation between low central entropy and presence of $H\alpha$ emission is very robust.

In Cavagnolo et al. (2008a) we present the result that the $K_0$ distribution for *ACCEPT* is bimodal. The clusters which populate the peak around $K_0 \approx 15$ keV cm$^2$ in that distribution are clusters with short central cooling times ($t_{\rm cool} \ll H_0^{-1}$) and would be classified as "cooling flow" clusters. Assuming star formation is associated with the $H\alpha$ nebulosity (Voit & Donahue 1997; Cardiel et al. 1998), it does not come as a surprise that modest star formation is occurring in these BCGs (Johnstone et al. 1987; McNamara & O'Connell 1989). But, it is very interesting that there appears to be a characteristic entropy threshold only below which multi-phase gas, and presumably stars, form. Voit et al. (2008) have recently proposed electron thermal conduction may be responsible for setting this threshold. This hypothesis has received further support from the theoretical work of Guo et al. (2008) showing that thermal conduction can stabilize non-cool core clusters against the formation of thermal instabilities.

## 4. RADIO SOURCES AND CENTRAL ENTROPY

Of the 217 clusters in *ACCEPT*, 97 have radio source detections with a mean $K_0$ of $22.8 \pm 9.2$ keV cm$^2$, while the other 120 clusters with only upper-limits have a mean $K_0$ of $130 \pm 51$ keV cm$^2$. Recall NVSS and SUMSS are low

[4] Faint Images of the Radio Sky at Twenty cm; http://sundog.stsci.edu

resolution surveys with FWHM at $\approx 45''$ which at $z = 0.2$ is $\approx 150$ kpc. This scale is larger then the size of a typical cluster cooling region and makes it difficult to determine absolutely that the radio emission is associated with the BCG. We therefore focus only on clusters at $z < 0.2$. After the redshift cut, 130 clusters remain – 61 with radio detections (mean $K_0 = 17.5 \pm 7.3$ keV cm$^2$) and 69 without (mean $K_0 = 107 \pm 44$ keV cm$^2$).

In Figure 2 we have plotted radio power versus $K_0$. The obvious dichotomy seen in the $H\alpha$ measures and characterized by $K_{\rm thresh}$ is also present in the radio as an overabundance of clusters with $\nu L_\nu \gtrsim 10^{40}$ erg s$^{-1}$ and $K_0 \lesssim K_{\rm thresh}$. This suggests that AGN activity in BCGs, while not exclusively limited to low core entropy clusters, is more likely to be found in clusters which have an average core entropy less than $K_{\rm thresh}$. That star formation and AGN activity are subject to the same entropy threshold before turning "on" suggests the mechanism which promotes or initiates one is also involved in the activation of the other. Our results also suggest that cold-mode accretion (Pizzolato & Soker 2005; Hardcastle et al. 2007) may be the dominant method of fueling AGN in BCGs.

We have again highlighted two subsets of clusters in Figure 2: clusters below $K_{\rm thresh}$ without radio sources (blue boxes with red stars) and clusters above $K_{\rm thresh}$ with radio sources (blue boxes with orange dots). The peculiar clusters below $K_{\rm thresh}$ are A133, A539, A1204, A2107, A2462, A2556, AWM7, ESO 5520200, MKW 04, and MS J1157.3+5531. The peculiar clusters above $K_{\rm thresh}$ are 2PIGG J0011.5-2850, A586, A2063, A2147, A2244, A3528S, A3558, A4038, and RBS 0461. Radio-quiet AGN are not uncommon, and having a few clusters in our sample without radio-loud sources where we expect to find them is not surprising. However, the clusters above $K_{\rm thresh}$ with a radio-loud source are interesting, and may be special cases of BCGs with embedded corona. Sun et al. (2007) extensively studied coronae and found they are like "mini-cooling cores" and may provide an environment insulated from the harsh ICM in which AGN fueling via cold gas blobs could proceed. Indeed, some of these peculiar clusters show indications that a very compact ($r \lesssim 5$ kpc) X-ray source is associated with the BCG. These peculiar clusters are most likely exceptions to the low entropy-AGN activity relation and do not weaken the overall trend.

## 5. SUMMARY

We have presented a comparison of ICM central entropy values and measures of BCG $H\alpha$ and radio emission for a *Chandra* archival sample of galaxy clusters. The mean $K_0$ for clusters with and without $H\alpha$ detections are $14.1 \pm 4.9$ keV cm$^2$ and $124 \pm 47$ keV cm$^2$, respectively. For clusters at $z < 0.2$ with BCG radio emission the mean $K_0 = 17.5 \pm 7.3$ keV cm$^2$, while for BCGs with only upper limits, the mean $K_0 = 107 \pm 44$ keV cm$^2$. We find that below a characteristic central entropy threshold of $K_0 \approx 30$ keV cm$^2$, $H\alpha$ and bright radio emission are more likely to be detected, while above this threshold $H\alpha$ is not detected and radio emission, if detected at all, is significantly fainter. While other mechanisms can produce $H\alpha$ or radio emission besides star formation and AGN, if one assumes the $H\alpha$ and radio emission are coming from these two feedback sources, then our results suggest the development of multiphase gas in cluster cores (from which stars could form and AGN could be feed) is strongly coupled to ICM entropy.

We were supported in this work through *Chandra* grants AR-6016X, AR-4017A, and NASA LTSA program NNG-05GD82G. The CXC is operated by the SAO for and on behalf of NASA under contract NAS8-03060.

## REFERENCES

Arnaud, K. A. 1996, in ASP Conf. Ser. 101: Astronomical Data Analysis Software and Systems V, ed. G. H. Jacoby & J. Barnes, 17–+
Bîrzan, L., Rafferty, D. A., McNamara, B. R., Wise, M. W., & Nulsen, P. E. J. 2004, ApJ, 607, 800
Bock, D. C.-J., Large, M. I., & Sadler, E. M. 1999, AJ, 117, 1578
Bower, R. G., Benson, A. J., Malbon, R., Helly, J. C., Frenk, C. S., Baugh, C. M., Cole, S., & Lacey, C. G. 2006, MNRAS, 370, 645
Burns, J. O. 1990, AJ, 99, 14
Burns, J. O., White, R. A., & Hough, D. H. 1981, AJ, 86, 1
Cardiel, N., Gorgas, J., & Aragon-Salamanca, A. 1998, MNRAS, 298, 977
Cavagnolo, K. W., Donahue, M., Sun, M., & Voit, G. M. 2008a, ApJ Submitted
Cavagnolo, K. W., Donahue, M., Voit, G. M., & Sun, M. 2008b, ArXiv e-prints, arxiv:0803.3858
Condon, J. J., Cotton, W. D., Greisen, E. W., Yin, Q. F., Perley, R. A., Taylor, G. B., & Broderick, J. J. 1998, AJ, 115, 1693
Cowie, L. L., Songaila, A., Hu, E. M., & Cohen, J. G. 1996, AJ, 112, 839
Crawford, C. S., Allen, S. W., Ebeling, H., Edge, A. C., & Fabian, A. C. 1999, MNRAS, 306, 857
Crawford, C. S., Hatch, N. A., Fabian, A. C., & Sanders, J. S. 2005, MNRAS, 363, 216
Croton, D. J., Springel, V., White, S. D. M., De Lucia, G., Frenk, C. S., Gao, L., Jenkins, A., Kauffmann, G., Navarro, J. F., & Yoshida, N. 2006, MNRAS, 365, 11
Donahue, M., Horner, D. J., Cavagnolo, K. W., & Voit, G. M. 2006, ApJ, 643, 730
Donahue, M., Stocke, J. T., & Gioia, I. M. 1992, ApJ, 385, 49
Donahue, M., Voit, G. M., O'Dea, C. P., Baum, S. A., & Sparks, W. B. 2005, ApJ, 630, L13
Guo, F., Oh, S. P., & Ruszkowski, M. 2008, ArXiv e-prints, arxiv:0804.3823
Hardcastle, M. J., Evans, D. A., & Croston, J. H. 2007, MNRAS, 376, 1849
Heckman, T. M., Baum, S. A., van Breugel, W. J. M., & McCarthy, P. 1989, ApJ, 338, 48
Johnstone, R. M., Fabian, A. C., & Nulsen, P. E. J. 1987, MNRAS, 224, 75
Juneau, S., Glazebrook, K., Crampton, D., McCarthy, P. J., Savaglio, S., Abraham, R., Carlberg, R. G., Chen, H.-W., Le Borgne, D., Marzke, R. O., Roth, K., Jørgensen, I., Hook, I., & Murowinski, R. 2005, ApJ, 619, L135
Kennicutt, Jr., R. C. 1983, ApJ, 272, 54
Kriss, G. A., Cioffi, D. F., & Canizares, C. R. 1983, ApJ, 272, 439
Lawrence, C. R., Zucker, J. R., Readhead, A. C. S., Unwin, S. C., Pearson, T. J., & Xu, W. 1996, ApJS, 107, 541
Mauch, T., Murphy, T., Buttery, H. J., Curran, J., Hunstead, R. W., Piestrzynski, B., Robertson, J. G., & Sadler, E. M. 2003, MNRAS, 342, 1117
McNamara, B. R., & Nulsen, P. E. J. 2007, ARA&A, 45, 117
McNamara, B. R., & O'Connell, R. W. 1989, AJ, 98, 2018
Pizzolato, F., & Soker, N. 2005, ApJ, 632, 821
Quillen, A. C., Zufelt, N., Park, J., O'Dea, C. P., Baum, S. A., Privon, G., Noel-Storr, J., Edge, A., Russell, H., Fabian, A., Donahue, M., Bregman, J. N., McNamara, B. R., & Sarazin, C. L. 2007, ArXiv e-prints, arxiv:0711.1118
Sun, M., Jones, C., Forman, W., Vikhlinin, A., Donahue, M., & Voit, M. 2007, ApJ, 657, 197
Valentijn, E. A., & Bijleveld, W. 1983, A&A, 125, 223
Valluri, M., & Anupama, G. C. 1996, AJ, 112, 1390
Voit, G. M. 2005, Reviews of Modern Physics, 77, 207
Voit, G. M., Bryan, G. L., Balogh, M. L., & Bower, R. G. 2002, ApJ, 576, 601
Voit, G. M., Cavagnolo, K. W., Donahue, M., Rafferty, D., & McNamara, B. 2008, ApJ Submitted
Voit, G. M., & Donahue, M. 1997, ApJ, 486, 242
White, D. A., Jones, C., & Forman, W. 1997, MNRAS, 292, 419